Hindawi
Geofluids
Volume 2023, Article ID 1444009, 11 pages
https://doi.org/10.1155/2023/1444009

Research Article

Analysis of Anisotropic Strength and Wellbore Unstable Zone in Shale Formation Relating to Water Content

Linjie Qiu,[1] **Min Zhang**,[2] **and Yansen Wang**[1]

[1]*State Key Laboratory for Geomechanics and Deep Underground Engineering, China University of Mining and Technology, Xuzhou, 221116 Jiangsu Province, China*
[2]*College of Mathematics, Sichuan University, Chengdu, 610000 Sichuan Province, China*

Correspondence should be addressed to Linjie Qiu; 15993738910@163.com and Yansen Wang; yswangcumt@126.com

Received 6 August 2022; Revised 22 October 2022; Accepted 24 November 2022; Published 8 February 2023

Academic Editor: Amin Gholami

During oil and gas exploitation, wellbore stability has always been the focus of many scholars. Instability of wellbore will lead to washouts, breakout, stuck pipe, mud loss, and so on, even the abandon of the well. Shale rock is widely distributed in nature and must be taken into account in some rock engineering applications. In order to evaluate the strength anisotropy and the influence of moisture content of the wellbore integrity, the LMX outcrops are divided into three groups to carry out triaxial strength experiment. Based on the fitting method of collaborative search, the strength parameters of different moisture contents are determined; then, the effect of strength anisotropy and the moisture content of the LMX reservoir on wellbore collapse pressure and wellbore integrity are investigated. The results show that shale strength, especially cohesion, is more sensitive to the influence of water. With the increase of water content, the inclination angle of the minimum value obtained by shale strength is deviated to the left, and the collapse pressure and instability area increase significantly. At the same time, it is necessary to adjust the direction of borehole drilling to avoid the occurrence of the zone of bedding slip instability in the direction of the minimum in situ stress, and the inversion of in situ stress should be corrected by considering the effect of bedding on the location of the maximum in situ stress. The study on the effects of bedding and water content on the instability zone can provide suggestions and guidance for the optimization of borehole trajectory, the control of bottom hole safety pressure, the inversion of in situ stress, and the drilling and completion of wells.

1. Introduction

Shale gas is an unconventional resource. The Silurian Longmaxi Formation shale in Sichuan Basin has a thickness of 65 m~516 m, which is an ideal horizon for exploration and development [1–3]. However, previous drilling experience and related research have found that the drilling complex conditions such as block drop, stuck, and collapse are frequent, leading to huge economic losses. Shale formation instability is an important issue to be considered in drilling operations [4, 5]. Therefore, it is necessary to explore the anisotropic strength and wellbore instability mechanism on the basis of laboratory experimental research and theoretical analysis.

Drilling workers at home and abroad have carried out a lot of research on wellbore stability in drilling, which can be divided into two aspects: stress distribution in near-wellbore zone and strength criterion of rock around the well. In order to evaluate the stress concentration state around the well after drilling, Westergaard [6] first gave an elastic-plastic stress distribution model around the well, but it required many parameters and was difficult to obtain. Therefore, the linear elastic borehole stress model with few demand parameters and convenient testing is widely used. Kirsch [7] first gave the linear elastic borehole stress model, but it is only applicable when the borehole points to the direction of the main in-situ stress. Fairhust [8] obtained for the first time a linear elastic borehole stress model for any well. Sedimentary rock can be considered transversely isotropic materials, the linear elastic parameters in vertical and parallel bedding direction significant difference, but the study shows that compared with the stress and the intensity, elastic anisotropic effect on borehole wall safe density window is very

limited [9–12], and the transverse isotropic well circumferential stress model only explains the sidewall of stress distribution. Therefore, this paper studies wellbore integrity based on the homogeneous linear elastic borehole stress model. The difference of strength with the change of the angle between bedding and load is a remarkable feature of shale research that is different from conventional reservoir research [13, 14]. Jaeger [15] proposed a weak plane strength theory for the first time based on MC strength theory and divided the failure of shale into two shear failure modes: body and weak plane, which can well explain the anisotropy of shale strength. It is widely used in borehole stability analysis. At present, direct shear experiments along the bedding plane or triaxial experiments of shale with an angle of 60° between normal and axial loads under different confining pressures are mostly used to obtain cohesion force and internal friction angle of the bedding plane [16–20]. However, the direct shear experiment only measured the cohesion force and internal friction angle of the bedding plane, and based on the shear experiment which was different from the failure mechanism of triaxial compression, the triaxial mechanical experiment assumed that the shale shear failure along the bedding plane with a bedding inclination of 60°, both of which failed to reflect the influence of bedding inclination on the continuous change of rock strength [21–24]. In addition, shale is characterized by fine layered structure, natural fractures, low permeability, and strong cation exchange capacity [25], which is sensitive to water-based mud, leading to serious wellbore instability. Therefore, oil-based mud is widely used, but the price of oil-based mud is high and it does great harm to the environment. When water-based drilling fluid is used to drill in shale formation, the influence of water on shale structure and mechanics must be mastered [26–28].

In order to study the influence of water content and bedding structure of shale on borehole stability, uniaxial and triaxial strength experiments were carried out on LMX shale with different confining pressures, inclination angle, and water content. The minimum root mean square error was used to fit all failure strength data. Based on the laboratory experimental parameters, a homogeneous linear elastic borehole stress model was adopted. The influence of water content and strength anisotropy on the instability area around shale wells is studied, and the borehole trajectory is optimized. The research results can provide suggestions for the use of water-based drilling fluid in shale gas wells and improve the actual drilling efficiency in the field.

2. Effect of Water Content on Shale Strength

2.1. Preparation and Experiment of Rock Samples. In general, shale has a certain degree of anisotropy and is isotropic in the direction of parallel planes but has different elastic characteristics in the vertical plane. When the shear failure occurs in the bedding plane, the strength of shale is significantly reduced, but when the shear failure occurs across the bedding plane, the strength increases [29, 30]. Figure 1 shows the schematic diagram of the relative angle between

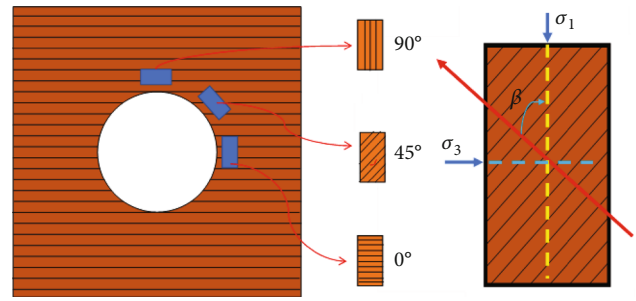

Figure 1: Schematic showing orientation of near-wellbore stress concentrations for horizontal well with respect to bedding orientations in layered formation [1].

the principal stress around the well and the normal relative angle of the surrounding rock. It can be seen that the angle between the principal stress around the well and the surrounding rock changes continuously from 0° to 90° along the well perimeter angle. Therefore, the collapse pressure at each point around the well is not only related to the well perimeter angle but also related to the strength of the stratum rock at the point.

A total of 84 standard shale samples with bedding inclination angle from 0° to 90° were drilled from the same rock mass taken from this formation, and the processing accuracy of rock samples met the requirement of "the maximum error of end surface roughness shall not exceed 0.02 mm, and the side roughness shall not exceed 0.3 mm" [31, 32]. The 84 samples were randomly divided into three groups, each containing the same number of cores with different bedding inclinations. After drying the cores, the samples of the second and third groups were placed in clean water at the same time, and the water-filling process was strictly according to the standard (ID: DZ/T0276.5-2015), take out the second group of samples after soaking for 24 h, and take out the third group of samples after soaking for 24 h. The moisture content of the three groups of samples after saturated experiment is shown in Figure 2.

The water content of shale samples after soaking for 24 h and 48 h is 0.594-0.738% and 0.909%-1.127%, respectively. Differences in moisture in the same set of samples may be due to different bedding orientations; further details of preparation and testing procedures are provided in reference 33, 34. After the water-saturation test, uniaxial and triaxial strength tests were carried out on the three groups of rock samples, respectively. The stress applied process was displacement loading, and the quasistatic loading state was maintained. The samples all failed within 5-15 min [35, 36].

2.2. Jaeger's Plane of Weakness Model. Most sedimentary rocks have anisotropic characteristics due to their special diagenetic processes, especially shale, which is more obvious. A lot of studies have been carried out on the anisotropic strength characteristics of shale, and a variety of prediction models have been established, but the same

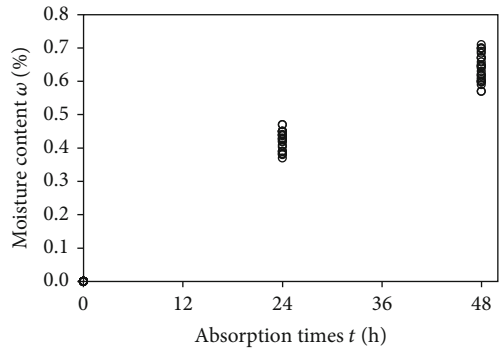

Figure 2: Moisture content of three groups of shales after different water absorption times [1].

evaluation method has not been formed so far. According to different classification criteria, it can be seen that the existing anisotropic strength criteria can be divided into different types, such as theoretical model and empirical relationship model according to the existence of theoretical basis. According to its envelope trend can be divided into shoulder type, U type, and wave type. According to its failure mode, it can be divided into continuous type and discontinuous type. The failure modes of stratified shale are divided into bulk shear failure and weak plane shear failure. Therefore, many scholars believe that the discontinuity criterion has clear physical significance and can better explain the instability mechanism of anisotropic rock. The weak surface criterion proposed by Zhang et al. [14] has been proved to conform to the anisotropic strength characteristics of most shale gas reservoirs in the world [23]. The physical concepts of cohesion and internal friction angle in the criterion are clear and mature in application in the petroleum industry. Therefore, this criterion is selected to fit the experimental data in this paper. The failure discriminant of body and bedding plane in Jaeger's weak surface criterion is shown as follows:

$$\sigma_1\text{-}\sigma_3 = 2(S_o + \sigma_3 \tan \phi_o)\left(\sqrt{1+\tan^2\phi_o} + \tan \phi_o\right), \quad (1)$$

$$\sigma_1\text{-}\sigma_3 == \frac{2\left(S_{bp} + \sigma_3 \tan \phi_{bp}\right)}{\left(1 - \tan\text{-}\phi_{bp} \tan \beta\right) \sin 2\beta}. \quad (2)$$

In which, σ_1 and σ_3 are maximum principal stress and minimum principal stress, respectively, MPa; S_o and S_{bp} are cohesion of shale rock matrix and bedding plane, MPa; ϕ_o and ϕ_{bp} are internal friction angle of shale rock matrix and bedding plane, deg; and β is the angle between the maximum principal stress and the normal direction of the weak plane, deg; as shown in Figure 1.

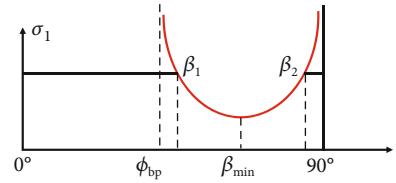

Figure 3: Jaeger' plane of weakness model failure envelops [24].

By analyzing Equations (1) and (2), it can be concluded that

$$\begin{cases} \beta_1 = \dfrac{\phi_{bp}}{2} + 0.5 \arcsin\left\{\dfrac{\left[\left(S_{bp}\cot\phi_{bp} + \sigma_m\right)\sin\phi_{bp}\right]}{\tau_m}\right\}, \\ \beta_2 = 90\circ + \dfrac{\phi_{bp}}{2} - 0.5 \arcsin\left\{\dfrac{\left[\left(S_{bp}\cot\phi_{bp} + \sigma_m\right)\sin\phi_{bp}\right]}{\tau_m}\right\}, \end{cases} \quad (3)$$

where σ_m and τ_m are the maximum normal stress and maximum shear stress, respectively, MPa; obviously, when β_1 is infinitely close to the internal friction angle ϕ_{bp} or β_2 is infinitely close to 90°, the core strength predicted by Equation (2) approaches infinity, as shown in Figure 3, according to Equation (3), when the minimum value of the available strength is obtained, the corresponding bedding angle is

$$\beta_{min} = \frac{(\beta_1 + \beta_2)}{2} = 45\circ + \frac{\phi_{bp}}{2}. \quad (4)$$

2.3. Strength Parameter Fitting. In order to predict the anisotropic strength of rock accurately, the strength parameters in the model must be determined by fitting the anisotropic failure experiment data accurately. In this paper, the minimum root mean square error is used, as shown in Equation (5), to get the optimal parameter [23]. The method can simultaneously determine the four strength parameters of the Jaeger weak surface criterion. First, the initial values of the undetermined parameters are given, and the cohesion force and internal friction angle of the body and the weak surface are set to vary within a wide range to ensure that the real values are within the range. When the RMSE of the predicted strength and laboratory strength data reaches the minimum value, the value at this time is the real core strength parameter. In the calculation process, the search accuracy can be increased appropriately to save the calculation time, and then, the search range is gradually reduced and the search accuracy is refined. After four or five cycles of solving, the intensity parameters with high accuracy are obtained [37, 38].

$$\text{RMSE} = \sqrt{\sum_{i=1}^{N} \frac{\left|\sigma_i^{\text{test}} - \sigma_i^{\text{predict}}\right|}{N}}. \quad (5)$$

In which, N is the number of experimental samples, σ_i^{test} is the tested strength of rock sample i, MPa; and $\sigma_i^{\text{predict}}$ is

the predicted strength of rock sample i, MPa. This method can obtain the cohesive force and internal friction angle which can best represent the failure strength of all confining pressures and dip samples and avoid the error caused by direct shear test or triaxial compression test with specific dip core. Taking the fitting of the strength data of rock samples soaked for 48 hours as an example, the cyclic iterative process of refining the search range of the four undetermined parameters in Jaeger's plane of weakness model is shown in Table 1.

As can be seen from Table 1, after three times of refinement of the search range, the accuracy of the intensity parameter can be improved to within 5%, and RMSE basically remains unchanged. The experimental strength data of LMX shale samples with different water contents is plotted in Figure 4, together with the predicted strength envelope of Jaeger's plane of weakness model. The strength of the shale rock increases with the increase of confining pressure and the decrease of water content. In addition, it decreases first with the increase of bedding dip angle, reaches the minimum value when the bedding inclination angle reaches 60°, and then increases gradually. Furthermore, it can be found that the strength of the vertical bedding plane ($\beta = 0°$) is greater than that of the parallel bedding plane ($\beta = 90°$). It is observed that the tensile cracks along the bedding plane appear in the core of the parallel bedding plane during the compression process, and the tensile strength of the rock is much smaller than the compressive strength, which is the main reason for the occurrence of this phenomenon. The MC criterion does not fully explain this characteristic of rock material, so Jaeger's plane of weakness model established based on the concept of cohesion and internal friction angle fails to distinguish the difference of shale strength parallel to the vertical bedding plane, but this criterion can reveal the variation trend of sample strength in the range of $\beta_1 \sim \beta_2$ accurately. Many studies have proved that this criterion has high accuracy in predicting the rock strength of most shale gas reservoirs in the world, and its application is mature in the petroleum industry. Therefore, this criterion is used as the judgment basis for wellbore integrity in this paper.

By analyzing the influence of water content on strength, it can be seen that the cohesion and internal friction angle of rock matrix are reduced in a small range, while the cohesion and internal friction angle of the bedding plane are significantly weakened; besides, the cohesion is more sensitive to the influence of water. The structure of shale rock matrix is compact and its permeability is very low, so it is difficult for water to enter the rock matrix; as a result, the cohesion and internal friction angle of the rock matrix have no obvious change with the increase of water content. However, microcracks develop in the bedding surface, which form a channel for water. Meanwhile, rich clay minerals develop in the bedding plane, which would soften, expand, and react with water, and then, the cohesion and internal friction angle are weakened. The analysis of the strength envelope of Jaeger's plane of weakness model also shows that, with the increase of water content, the position where the strength reaches the lowest point gradually shifts to the left. If only the strength of rock sample with $\beta = 60°$ is tested, the strength of the shale rock with different bedding dips will be overestimated, which will lead to the frequent occurrence of complex situations in drilling engineering.

The failure of anisotropic shale not only depends on the hydrostatic environment and loading direction but also depends on the water content. The water evaporation of cored rock will lead to the increase of shale strength. Influence of these factors should be considered in the analysis of engineering application.

3. Wellbore Stability Prediction Model

After the formation is drilled, the in situ stress is redistributed around the borehole, and the drilling fluid column pressure replaces the drilled rock to support the borehole wall, and the stress balance is reached again. In order to obtain the distribution of the stress around the borehole, the ground stress should be first converted to geodetic coordinates and then from geodetic coordinates to borehole cartesian coordinate system. Finally, the borehole stress distribution model in polar coordinates is obtained [10]. Under the plane strain condition, the stress component around the well in borehole polar coordinate system [10] is shown in

$$
\begin{cases}
\sigma_r = \dfrac{(\sigma_{xx}+\sigma_{yy})}{2}\left(1-\dfrac{r_w^2}{r^2}\right) + \dfrac{(\sigma_{xx}-\sigma_{yy})}{2}\left(1-4\dfrac{r_w^2}{r^2}+3\dfrac{r_w^4}{r^4}\right)\cos 2\theta + \tau_{xy}\left(1-4\dfrac{r_w^2}{r^2}+3\dfrac{r_w^4}{r^4}\right)\sin 2\theta + P_w\dfrac{r_w^2}{r^2} - \alpha P_p, \\
\sigma_\theta = \dfrac{(\sigma_{xx}+\sigma_{yy})}{2}\left(1+\dfrac{r_w^2}{r^2}\right) - \dfrac{(\sigma_{xx}-\sigma_{yy})}{2}\left(1+3\dfrac{r_w^4}{r^4}\right)\cos 2\theta + \tau_{xy}^b\left(1+3\dfrac{r_w^4}{r^4}\right)\sin 2\theta - P_w\dfrac{r_w^2}{r^2} - \alpha P_p, \\
\sigma_z = \sigma_z^b - 2\nu(\sigma_{xx}-\sigma_{yy})\dfrac{r_w^2}{r^2}\cos 2\theta - 4\nu\tau_{xy}\dfrac{r_w^2}{r^2}\sin 2\theta - \alpha P_p, \\
\tau_{r\theta} = \left[\dfrac{(\sigma_{xx}+\sigma_{yy})}{2}\sin 2\theta + \tau_{xy}^b\cos 2\theta\right]\left(1+2\dfrac{r_w^2}{r^2}-3\dfrac{r_w^4}{r^4}\right), \\
\tau_{rz} = \left[\tau_{yz}\sin\theta + \tau_{xz}\cos\theta\right]\left(1-\dfrac{r_w^2}{r^2}\right), \\
\tau_{\theta z} = \left[-\tau_{xz}\sin\theta + \tau_{yz}\cos\theta\right]\left(1+\dfrac{r_w^2}{r^2}\right),
\end{cases}
\tag{6}
$$

Table 1: Example of Iterative process for Jaeger's plane of weakness model.

Procedure	Undetermined parameters So (MPa)	fo (deg)	S_{bp} (MPa)	f_{bp} (deg)	Calculation accuracy ($i = 1:1:20$)	RMSE (MPa)
1	41	40	28	27	$So = 4^*(i) + 5$, $fo = 2^*(i) + 10$, $S_{bp} = 4^*(i)$, $f_{bp} = 2^*(i) + 5$	30.5819
2	42	39	29.5	26.8	$So = 0.5^*(i) + 36.5$, $fo = 0.5^*(i) + 35.5$, $S_{bp} = 0.5^*(i) + 23.5$, $f_{bp} = 0.2^*(i) + 24.8$	30.2728
3	41.6	39.2	29.45	26.85	$So = 0.05^*(i) + 41.45$, $fo = 0.05^*(i) + 38.45$, $S_{bp} = 0.05^*(i) + 28.95$, $f_{bp} = 0.05^*(i) + 26.25$	30.2708

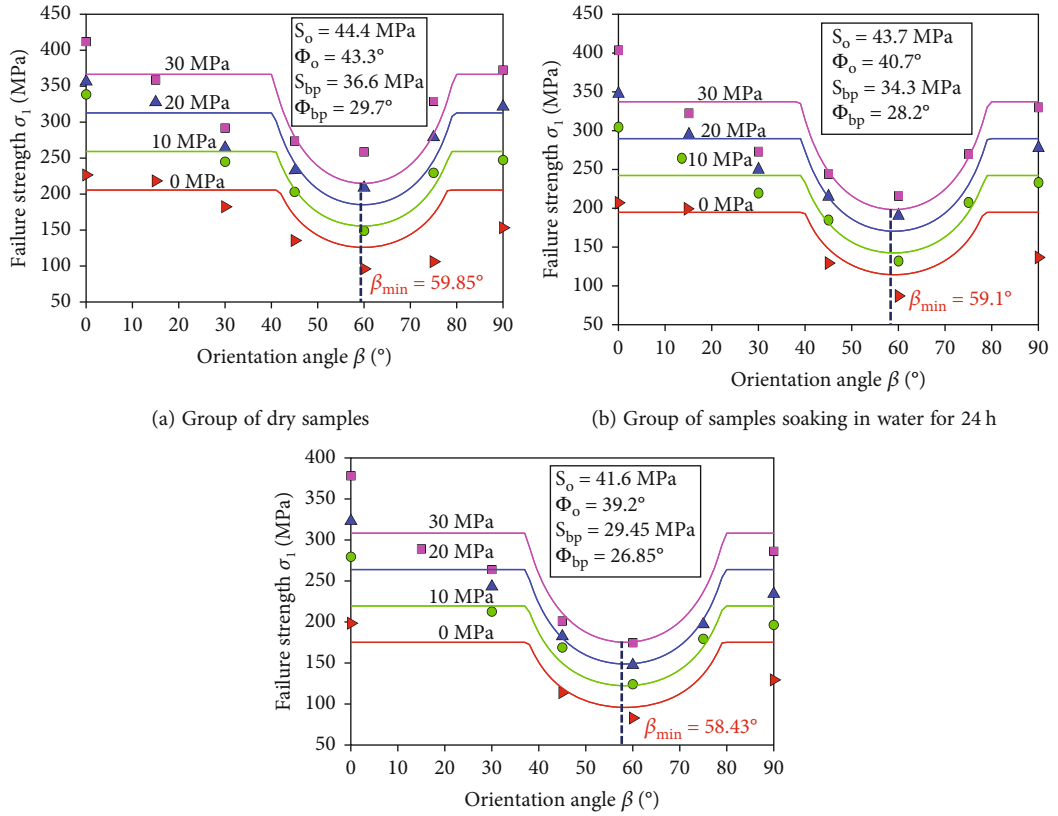

(a) Group of dry samples

(b) Group of samples soaking in water for 24 h

(c) Group of samples soaking in water for 48 h

Figure 4: Experimental data with different moisture content fit by plane of weakness model.

where r_w is the wellbore radius, mm; r is the distance between a point in the formation and the axis of the wellbore, mm; θ is the wellbore circumference angle, i.e., the angle with the axis $\mathbf{X_b}$ in the clockwise direction, °; and P_w and P_p are the wellbore fluid column pressure and formation pore pressure, respectively, MPa.

Different from the isotropic strength model, shale anisotropic strength criterion in addition to the strength parameters and confining pressure, also associated with variable bedding angle, should be determined in the borehole wall stability analysis well weeks each point of maximum principal stress and the stratification plane to the angle, but the determination of the maximum principal stress direction well weeks is not intuitive, in the process of solving the wellbore collapse pressure. The minimum principal stress around the well is the bottom hole fluid column pressure or radial stress, which is easier to obtain in the geodetic coordinate system. As shown in Figure 1, the angle between the minimum principal stress around the well and the normal of the bedding plane can be obtained, and the former is complementary to the angle. After obtaining the direction vectors of normal bedding plane and radial stress around well in geodetic coordinates, the angle between them can be obtained.

The occurrence of the bedding plane in the geodetic coordinate system is shown in Figure 5, and α_{bp} and β_{bp} are dipping direction and dipping angle of bedding plane, respectively, deg; the axis $\mathbf{Z_{bp}}$ are the normal direction of bedding plane. After mathematical derivation, the normal vector of bedding plane can be expressed as

$$\vec{\mathbf{n}} = \left[\cos\alpha_{bp}\sin\beta_{bp}, \sin\alpha_{bp}\sin\beta_{bp}, \cos\beta_{bp}\right]. \quad (7)$$

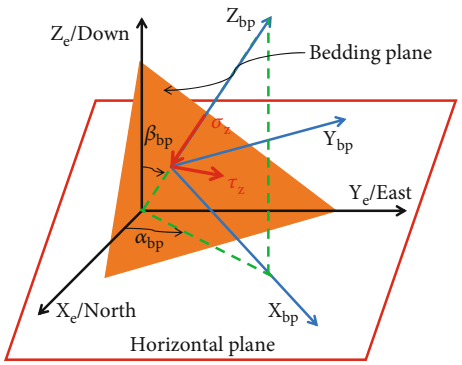

Figure 5: Reference coordinate systems of BPCS and GCS [1].

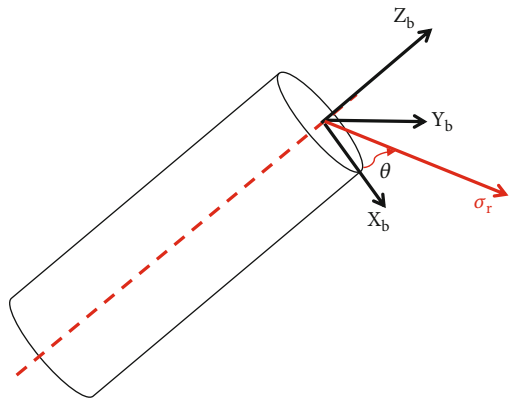

Figure 6: Reference coordinate systems of BPCS and GCS.

As shown in Figure 6, the minimum principal stress at a point around the borehole wall is radial stress σ_r; the axis $\mathbf{X_b}$ of the borehole rectangular coordinate system rotates by a certain angle with $\mathbf{Z_b}$ as the rotation axis, which is the direction of the minimum principal stress. The coordinate transformation process from the axis $\mathbf{X_b}$ to the direction of minimum principal stress is shown in

$$\vec{\mathbf{N}} = \begin{bmatrix} \cos\theta & \sin\theta & 0 \\ -\sin\theta & \cos\theta & 0 \\ 0 & 0 & 1 \end{bmatrix} \cdot \overrightarrow{\mathbf{X_b}} = \begin{bmatrix} \cos\alpha_b \cos\beta_b \cos\theta + \sin\alpha_b \cos\beta_b \sin\theta \\ -\cos\alpha_b \cos\beta_b \sin\theta + \sin\alpha_b \cos\beta_b \cos\theta \\ -\sin\beta_b \end{bmatrix}. \tag{8}$$

In which, the vector direction of axis $\mathbf{X_b}$ is expressed as follows:

$$\overrightarrow{\mathbf{X_b}} = [\cos\alpha_b \cos\beta_b, \sin\alpha_b \cos\beta_b, -\sin\beta_b]. \tag{9}$$

The sine of the normal vector of the bedding plane and the minimum principal stress vector around the well is the angle between the normal of the bedding plane and the maximum principal stress direction,

$$\beta = \arcsin \frac{\vec{\mathbf{n}}\vec{\mathbf{N}}}{\left|\vec{\mathbf{n}}\right|\left|\vec{\mathbf{N}}\right|}. \tag{10}$$

Since the strength model is usually expressed in the form of principal stress, the principal stress around the well can be obtained by substituting the stress component around the well into

$$\begin{cases} \sigma_{1,2} = \dfrac{\sigma_\theta + \sigma_z}{2} \pm \sqrt{\dfrac{(\sigma_\theta + \sigma_z)^2 + 4\tau_{\theta z}^2}{2}}, \\ \sigma_3 = \sigma_r. \end{cases} \tag{11}$$

By substituting Equations (10) and (11) into Jaeger's plane of weakness model, the stable state of each point around the well can be judged. Considering the periodicity and symmetry of the circular angle, its value range was set as 0° to 180° in the subsequent analysis, with a given increment of 2°. The variation range of hole inclination angle was set to be 0°~90° with an interval of 5°. The variation range of hole azimuth was set to be 0°~360° with an interval of 10°. The collapse pressure at borehole wall for the well with arbitrary trajectory (α_b, β_b) can be obtained by setting $r = r_w$ through Newton iteration algorithm. If $r > r_w$ is set, the stability of wellbore surrounding rock at the position r away from the axis of borehole can be judged.

4. Study on Characteristics of Wellbore Instability

4.1. Effect of Moisture Content on Unstable Region. Taking the shale of Lower Silurian LMX Formation in CN block, Sichuan Basin as an example, the wellbore stability is analyzed. In the CN block, the vertical crustal stress is 136.4 MPa, the maximum horizontal crustal stress is 155.0 MPa, the minimum horizontal crustal stress is 117.8 MPa, and the formation pressure is 82.5 MPa. The in situ stress is a typical strike-slip mechanism. Biot effective stress coefficient is 0.8, and the dipping direction of bedding plane is N150°E; that is, along the horizontal direction of maximum in-situ stress, the dipping angle of bedding plane is 1.2°. The practice has proved that the wellbore instability accident does not necessarily occur after the shear failure of the rock around the well. However, the study on the drilling fluid density to maintain the wellbore stability and the instability area around the well is still rare when the shear caving of the rock around the well is allowed within a certain range. In addition, a large number of directional microcracks develop along the bedding plane of shale, and simply treating them as isotropic cannot describe the actual problem. It has also been proved in practical drilling projects that the collapse pressure of shale borehole wall predicted by conventional models causes serious borehole expansion phenomenon. Therefore, how to obtain the influence of strength anisotropy on the stability of rock around the well and how to obtain the instability region around the well and optimize the well trajectory according to the method needs to be solved urgently.

The horizontal well drilling along the maximum horizontal principal stress in the CN block is analyzed. Assuming that the bottom hole pressure is 63.0 MPa, the instability region around the well with different water

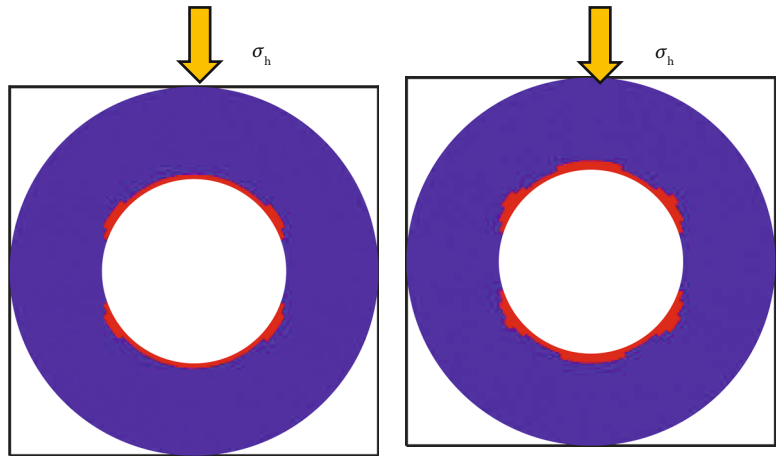

(a) The dry core (b) The core is soaked for 24 h

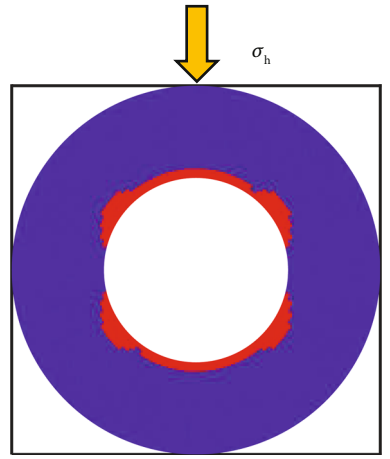

(c) The core is soaked for 48 h

Figure 7: Polar plots of shale gas well collapse pressure under different moisture contents.

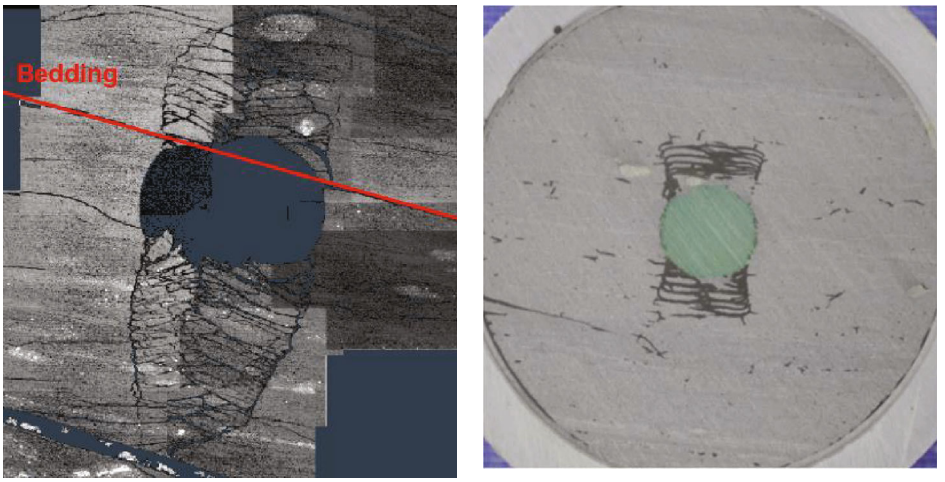

(a) Laboratory tests of wellbore instability in shale formations conducted by Økland and Cook [31]

(b) Laboratory tests of wellbore instability in shale formations conducted by Bautmans et al. [32]

Figure 8: Collapse mechanism in a thick-walled cylinder test performed with well oriented parallel to bedding.

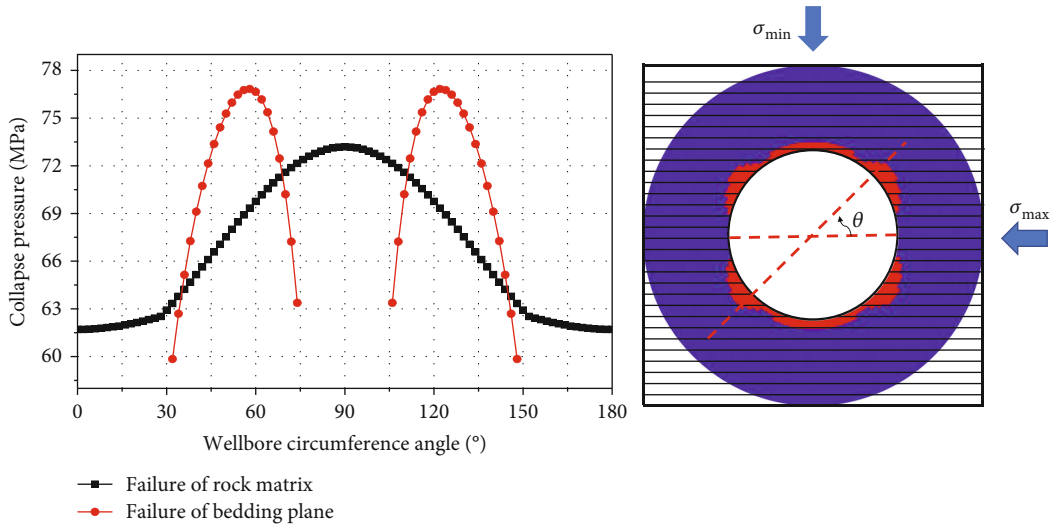

(a) The dipping angle of bedding plane is 0°

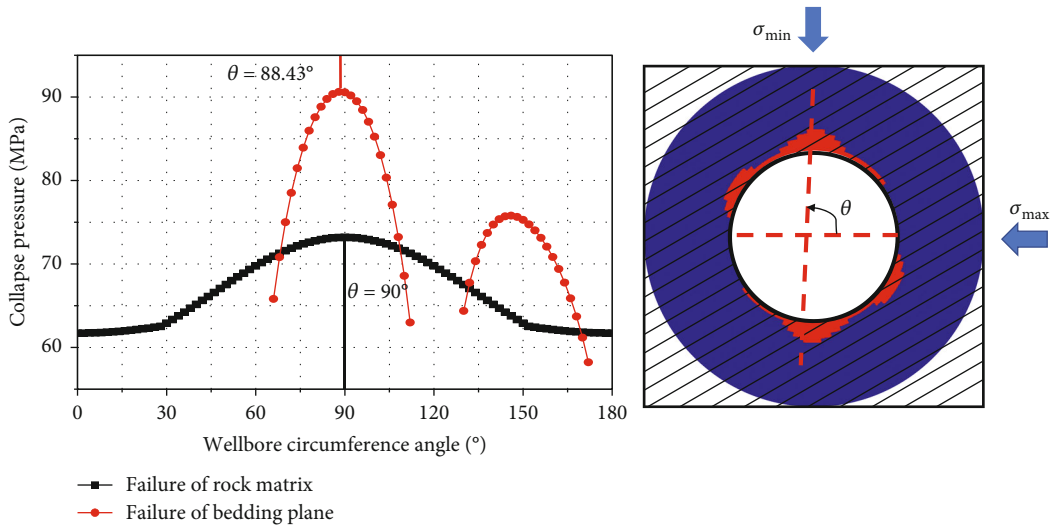

(b) The dipping angle of bedding plane is 30°

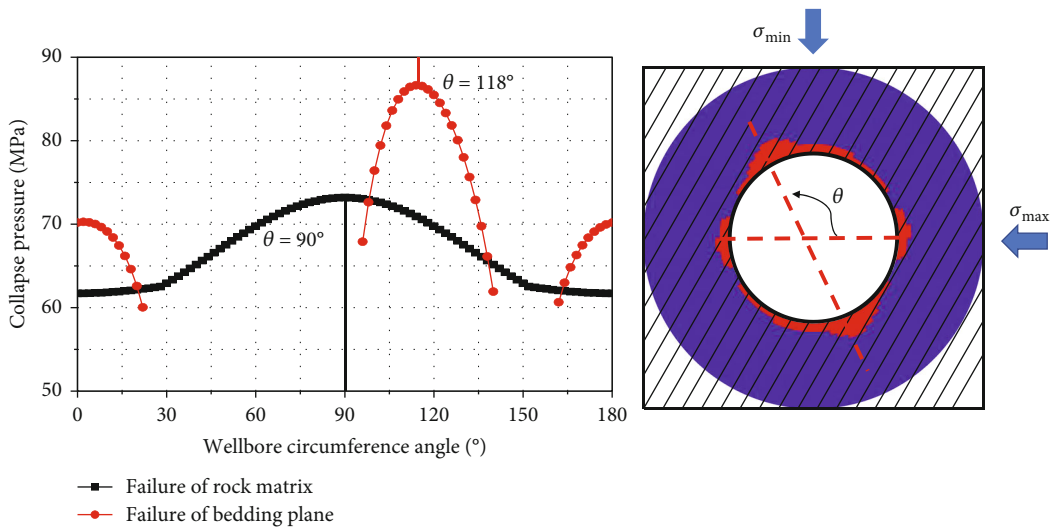

(c) The dipping angle of bedding plane is 60°

Figure 9: Polar plots of shale gas well collapse pressure under different moisture contents.

contents is shown in Figure 7. It can be seen that after considering the influence of the weak plane, the predicted wellbore shape becomes "quadrilateral." The instability region is not only concentrated in the direction of the minimum principal stress but also distributed on the left and right sides of the wellbore. With the increase of water content, the instability region gradually increases, which shows that with the extension of the contact time between the formation and drilling fluid, the water content gradually increases; especially in the late drilling stage, the risk of wellbore instability will increase significantly. It is necessary to strengthen the plugging characteristics of drilling fluid, slow down the intrusion of fluid into the bedding surface, and prevent the accumulation of caving cuttings at the bottom of the well by increasing the displacement.

4.2. Influence of Bedding Occurrence on Wellbore Collapse Orientation. Økland and Cook [31] and Bautmans et al. [32] had carried out the shale formations such as horizontal well instability condition of indoor simulation test, as shown in Figure 8, in the drilling process of the bedding plane developed shale formation, instability of regional distribution in wellbore at both ends up and down, and the well surrounding rock mainly occurred along the bedding surface caving. In view of this phenomenon, the author uses the model established in this paper to study the instability region of horizontal wells drilled in shale formations with different bedding inclination angles.

It is assumed that a well in the CN block is drilled with maximum in situ stress, and the mud pressure at the bottom of the well is 63.00 MPa. The shale strength parameters are shown in Figure 4(c), and only the bedding plane inclination angle is changed. When the inclination angle is 0°, 30°, and 60°, the collapse pressure at the borehole wall and the instability region around the well in the range of $r_w \sim 2r_w$ are shown in Figure 9. It can be seen that with the increase of bedding plane inclination angle, the collapse pressure of shale body remains unchanged on the borehole wall and reaches the maximum value at the borehole circumference angle of 90°, and the maximum instability region occurs in the direction of the minimum principal stress. However, the bottom hole pressure to maintain bedding plane stability has changed greatly, and the maximum instability area around the well and the horizontal maximum in situ stress have gradually increased. When the bedding plane dip angle is 30°, the sliding instability area caused by the weak plane and the shear failure instability area of the rock matrix are superimposed together, resulting in the increase of wellbore instability depth and further deterioration of wellbore stability. It is necessary to adjust the wellbore trajectory in the drilling process to avoid this situation.

In isotropic formation, wellbore collapse occurs in the direction of minimum in situ stress, but in stratified shale formation, the location of caving changes due to the anisotropy of rock strength around the well. If the strength anisotropy is not considered, the inversion of in situ stress based on the caving location of the shaft wall will have serious deviation. According to the three situations in Figure 9, it can be found that the direction of failure region for the well drilled along the direction of the horizontal maximum in situ stress is in the point $\theta = \beta_{bp} + \beta_{min}$. There is a certain angle between the maximum caving position and the direction of the minimum principal stress around the wellbore obtained by the wellbore instability region model considering the influence of weak plane [14]. According to this phenomenon, the inversion results of in-situ stress of shale reservoir can be corrected.

5. Conclusions

Through the above research, the following can be found:

(1) The strength parameters of shale bedding surface, especially cohesion, are more sensitive to the influence of water, while the shale body structure is compact and the permeability of water is weak, so its strength is less affected by water. The increase of water content will also lead to a shift of the bedding inclination angle to the left when the shale strength reaches the lowest value. The anisotropy of shale strength is controlled by confining pressure, bedding inclination angle, and water content

(2) Due to abundant bedding planes developed in shale, it is easy to form a "quadrilateral" well after drilling. The instability area is not only concentrated in the direction of the minimum principal stress but also distributed on the left and right sides of the well

(3) The position and depth of the maximum instability zone also change with the increase of the inclination angle of the bedding, and the superposition of the bedding sliding instability zone and the bulk shear instability zone will further deteriorate the wellbore stability. Therefore, the zone of bedding instability should be prevented from occurring in the direction of the horizontal minimum principal stress

Data Availability

All the data used to support the findings of this study are included within the article.

Conflicts of Interest

The authors declare that there is no conflict of interest regarding the publication of this paper.

Acknowledgments

This work was supported by the National Natural Science Foundation of China (Grant no. 52074264 and Grant no. 51174194), the National Key Research and Development Program of China (Grant no. 2016YFC0600903), and the Fundamental Research Funds for the Central Universities of China (Grant no. 2018ZZCX04 and Grant no. 2021 GJZPY15).

References

[1] D. I. Yi, L. I. Xiangjun, and L. U. Pingya, "Research on wellbore stability for hard brittle shale," *China Offshore Oil and Gas*, vol. 30, no. 1, pp. 142–149, 2018.

[2] Y. Xia, H. Wen, Y. Jin, M. Chen, and Y. Lu, "Poroelasto dynamic response of a wellbore to unloading in a formation under non-hydrostatic in-situ stresses," *Chinese Journal of Rock Mechanics and Engineering*, vol. 37, no. 5, pp. 1115–1125, 2018.

[3] W. B. Bradley, "Failure of inclined boreholes," *Journal of Energy Resources Technology*, vol. 101, no. 4, pp. 232–239, 1979.

[4] S. M. Willson, S. T. Edwards, A. Crook et al., "Assuring stability in extended reach wells-analyses, practices and mitigations," in *SPE/IADC Drilling Conference*, Society of Petroleum Engineers, 2007.

[5] L. Liang, L. Zhou, X. Liu, and Q. Chen, "Study of effect of pore structure on ultrasonic attenuation," *Chinese Journal of Rock Mechanics and Engineering*, vol. 34, no. S1, pp. 3208–3214, 2015.

[6] H. M. Westergaard, "Plastic state of stress around a deep well," *Journal of the Boston Society of Civil Engineers*, vol. 27, pp. 1–5, 1940.

[7] C. Kirsch, "Die theorie der elastizitat und die bedurfnisse der festigkeitslehre," *Zeitschrift des Vereines Deutscher Ingenieure*, vol. 42, pp. 797–807, 1898.

[8] C. Fairhurst, *Methods of Determining In-Situ Rock Stresses at Great Depths*, Missouri River Division US Army, Corps of Engineers, 1967.

[9] S. H. Ong and J. C. Roegiers, "Horizontal wellbore collapse in an anisotropic formation," in *SPE Production Operations Symposium*, Society of Petroleum Engineers, 1993.

[10] M. Zhang, L. Liang, and X. Liu, "Impacts of rock anisotropy on horizontal wellbore stability in shale reservoir," *Applied Mathematics and Mechanics*, vol. 38, no. 3, pp. 295–309, 2017.

[11] Y. K. Lee, S. Pietruszczak, and B. H. Choi, "Failure criteria for rocks based on smooth approximations to Mohr-Coulomb and Hoek-Brown failure functions," *International Journal of Rock Mechanics and Mining Sciences*, vol. 56, pp. 146–160, 2012.

[12] L. Huang, M. Yu, S. Miska, N. Takach, and J. B. Bloys, "Parametric sensitivity study of chemo-poro-elastic wellbore stability considering transversely isotropic effects in shale formations," in *SPE Canadian Unconventional Resources Conference*, Society of Petroleum Engineers, 2012.

[13] A. A. Alqahtani, M. Mokhtari, A. N. Tutuncu, and S. Sonnenberg, "Effect of mineralogy and petrophysical characteristics on acoustic and mechanical properties of organic rich shale," in *Unconventional Resources Technology Conference*, pp. 399–411, Denver Colorado USA, 2013.

[14] Q. Zhang, W. Jia, X. Fan, Y. Liang, and Y. Yang, "A review of the shale wellbore stability mechanism based on mechanical-chemical coupling theories," *Petroleum*, vol. 1, no. 2, pp. 91–96, 2015.

[15] J. C. Jaeger, "Shear failure of anistropic rocks," *Geological Magazine*, vol. 97, no. 1, pp. 65–72, 1960.

[16] J. Zhang, "Borehole stability analysis accounting for anisotropies in drilling to weak bedding planes," *International Journal of Rock Mechanics and Mining Sciences*, vol. 60, no. 2, pp. 160–170, 2013.

[17] P. Chen, T. Ma, and H. Xia, "A collapse pressure prediction model for horizontal shale gas wells with multiple weak planes," *Natural Gas Industry B*, vol. 2, no. 1, pp. 101–107, 2015.

[18] Y. Ding, P. Luo, X. Liu, and L. Liang, "Wellbore stability model for horizontal wells in shale formations with multiple planes of weakness," *Journal of Natural Gas Science and Engineering*, vol. 52, pp. 334–347, 2018.

[19] Y. H. Lu, M. Chen, Y. Jin, W. F. Ge, S. An, and Z. Zhou, "Influence of porous flow on wellbore stability for an inclined well with weak plane formation," *Petroleum Science and Technology*, vol. 31, no. 6, pp. 616–624, 2013.

[20] J. Zhou, S. He, M. Tang et al., "Analysis of wellbore stability considering the effects of bedding planes and anisotropic seepage during drilling horizontal wells in the laminated formation," *Journal of Petroleum Science and Engineering*, vol. 170, pp. 507–524, 2018.

[21] M. Liu, Y. Jin, Y. Lu et al., "A wellbore stability model for a deviated well in a transversely isotropic formation considering poroelastic effects," *Rock Mechanics and Rock Engineering*, vol. 49, no. 9, pp. 3671–3686, 2016.

[22] W. G. Pariseau, "Plasticity theory for anisotropic rocks and soil," in *In the 10th US Symposium on Rock Mechanics (USRMS)*, American Rock Mechanics Association, 1968.

[23] E. Hoek and E. T. Brown, "Empirical strength criterion for rock masses," *Journal of Geotechnical and Geoenvironmental Engineering*, vol. 106, no. 9, pp. 1013–1035, 1980.

[24] J. Ambrose, R. W. Zimmerman, and R. Suarez-Rivera, "Failure of shales under triaxial compressive stress," in *In 48th US Rock Mechanics/Geomechanics Symposium*, American Rock Mechanics Association, 2014.

[25] M. Zhang, X. Fan, Q. Zhang et al., "Parametric sensitivity study of wellbore stability in transversely isotropic medium based on polyaxial strength criteria," *Journal of Petroleum Science and Engineering*, vol. 197, article 108078, 2021.

[26] M. Borsetto, S. Martinetti, and R. Ribacchi, "Interpretation of in situ stress measurements in anisotropic rocks with the door-stopper method," *Rock Mechanics and Rock Engineering*, vol. 17, no. 3, pp. 167–182, 1984.

[27] Y. H. Abousleiman, J. C. Roegiers, L. H. Cui, and A. D. Cheng, "Poroelastic solution of an inclined borehole in a transversely isotropic medium," in *In the 35th US Symposium on Rock Mechanics (USRMS)*, American Rock Mechanics Association, 1995.

[28] G. Chen and R. T. Ewy, "Thermoporoelastic effect on wellbore stability," *SPE Journal*, vol. 10, no. 2, pp. 121–129, 2005.

[29] M. Zhang, L. Liang, and X. Liu, "Impact analysis of different rock shear failure criteria to wellbore collapse pressure," *Chinese Journal of Rock Mechanics and Engineering*, vol. 36, no. S1, pp. 372–378, 2017.

[30] J. Gao, J. Deng, K. Lan, Z. Song, Y. Feng, and L. Chang, "A porothermoelastic solution for the inclined borehole in a transversely isotropic medium subjected to thermal osmosis and thermal filtration effects," *Geothermics*, vol. 67, pp. 114–134, 2017.

[31] D. Økland and J. M. Cook, "Bedding-related borehole instability in high-angle wells," in *SPE/ISRM Rock Mechanics in Petroleum Engineering*, Society of Petroleum Engineers, 1998.

[32] P. Bautmans, E. Fjær, and P. Horsrud, "The effect of weakness patches on wellbore stability in anisotropic media," *International Journal of Rock Mechanics and Mining Sciences*, vol. 104, pp. 165–173, 2018.

[33] A. Mirahmadizoghi, *Analysis of rock performance under three-dimensional stress to predict instability in deep boreholes*, The University of Adelaide, 2012, Doctoral dissertation,.

[34] M. Zhang, X. Fan, Q. Zhang et al., "Influence of multi-planes of weakness on unstable zones near wellbore wall in a fractured formation," *Journal of Natural Gas Science and Engineering*, vol. 93, p. 104026, 2021.

[35] M. Chen, C. W. Zang, Z. W. Ding et al., "Effects of confining pressure on deformation failure behavior of jointed rock," *Journal of Central South University*, vol. 29, no. 4, pp. 1305–1319, 2022.

[36] Q. Feng, J. Jin, S. Zhang, W. Liu, X. Yang, and W. Li, "Study on a damage model and uniaxial compression simulation method of frozen-thawed rock," *Rock Mechanics and Rock Engineering*, vol. 55, no. 1, pp. 187–211, 2022.

[37] Y. Xue, P. G. Ranjith, Y. Chen, C. Cai, F. Gao, and X. Liu, "Nonlinear mechanical characteristics and damage constitutive model of coal under CO2 adsorption during geological sequestration," *Fuel*, vol. 331, p. 125690, 2023.

[38] Y. Xue, J. Liu, P. G. Ranjith, F. Gao, H. Xie, and J. Wang, "Changes in microstructure and mechanical properties of low-permeability coal induced by pulsating nitrogen fatigue fracturing tests," *Rock Mechanics and Rock Engineering*, vol. 55, no. 12, pp. 7469–7488, 2022.